Modeling the HDO Cycle with a Global Climate Model During the MY34 "Dusty" Season

Margaux Vals, Loïc Rossi, Franck Montmessin, Franck Lefèvre, Francisco Gonzalez-Galindo, Anna A. Fedorova, Mikhail Luginin, François Forget, Ehouarn Millour, Oleg I. Korablev, et al.

HAL Id: insu-03749347

https://insu.hal.science/insu-03749347

Submitted on 10 Aug 2022

MODELING THE HDO CYCLE WITH A GLOBAL CLIMATE MODEL DURING THE MY34 "DUSTY" SEASON.

M. Vals, *(margaux.vals@latmos.ipsl.fr)*, **L. Rossi, F. Montmessin, F. Lefèvre,** *Laboratoire ATmosphères, Milieux, Observations Spatiales, Paris, Guyancourt, France*, **F. Gonzalez-Galindo,** *Instituto de Astrofísica de Andalucía-CSIC, Granada, Spain*, **A. Fedorova, M. Luginin,** *Space Research Institute (IKI), Moscow, Russia*, **F. Forget, E. Millour,** *Laboratoire de Météorologie Dynamique, Paris, France*, **O. Korablev, A. Trokhimovskiy, A. Shakun,** *Space Research Institute (IKI), Moscow, Russia*, **A. Bierjon,** *Laboratoire de Météorologie Dynamique, Paris, France*, **L. Montabone,** *Laboratoire de Météorologie Dynamique, Paris, France*, *Space Science Institute, Boulder, CO, USA*.

Introduction

The D/H ratio observed in a planetary atmosphere is a proxy for the ratio of the current water reservoir over the initial water reservoir of the planet. The current D/H ratio measured in the Martian atmosphere is at least five times that of the Vienna Standard Mean Ocean Water (VSMOW) [1],[2],[3],[4]. This high value of the martian D/H ratio, derived from the HDO/H_2O abundance ratio, is a precious indicator of the large escape of water from the martian atmosphere along time. Apart from the mass difference between both isotopes, the differential escape of H and D comes from the preferential photolysis of H_2O over HDO [5] and the Vapor Pressure Isotope Effect (VPIE) that produces an isotopic fractionation at condensation [6],[7],[8]. Modeling the HDO cycle and the different processes, which lead to the D/H ratio at escape in the upper atmosphere, is key to understand the history of water in the Martian atmosphere. Rossi et al. 2021 [9] have implemented the HDO cycle in the updated version of the LMD Mars Global Climate Model (GCM) [10], based on previous work conducted by Montmessin et al. 2005 [11] accounting for the fractionation by condensation. The NOMAD and ACS instruments onboard ExoMars Trace Gas Orbiter (TGO) spacecraft have recently provided unprecedented observations of the HDO amount and D/H ratio profiles in the martian atmosphere [12],[13],[14],[15], motivating models development and validation [9],[16]. In particular, TGO data cover the second half, commonly named the "dusty season", of the martian year (MY) 34, which includes a Global Dust Storm (GDS) (Ls 180-230°) and a regional dust storm (Ls 315-330°). These exceptional events have been proven to be of particular importance in the hygrogen escape inventory, as the large load of dust in the atmosphere leads to an increase of temperature, which fosters the transport of water vapor to the upper atmosphere [12],[17],[18],[19],[20].

HDO modeling

Using previous work by Montmessin et al. 2005[11], Rossi et al. 2021[9] have introduced the representation of the HDO cycle in the LMD Mars Global Climate Model (GCM)[10]. In this last version of the model, dust is represented by a semi-interactive scheme[21], which simultaneously allows the free evolution of the vertical distribution of dust, going through the different physical parametrizations, and ensures the match of the integrated column dust opacity to the observed values, as compiled by Montabone et al. 2015,2020[22],[23], for the radiative transfer calculations. In this context, the same simplified cloud model version as in Montmessin et al. (2005)[11] was used, meaning water vapor is turned into ice as soon as saturation is reached. Vals et al. 2022[24] have recently adapted these implementations to the complete representation of the water ice clouds, including microphysics and radiative effect of clouds [25],[26]. Microphysics refer to the parametrization of the different processes of formation of the clouds such as nucleation of the ice particles on dust particles, water ice growth and dust scavenging implemented in the model by Navarro et al. 2014[26] and necessary to allow the occurrence of supersaturation in the model. The effect of kinetics in the fractionation by condensation process, relying on the difference of diffusion of HDO and H_2O molecules in a saturated atmosphere, has also been included, so as the photodissociation of HDO and the photochemical reactions of the deuterated species, implemented in the model by F. Lefèvre and F. Gonzalez-Galindo, based on [27],[28],[29], accounting for the effect of fractionation by photolysis.

Model sensitivity to physical parametrizations

In Vals et al. 2022[24], GCM simulations are confronted to temperature, H_2O and saturation occultation profiles derived from the TGO/ACS instrument provided by A. Fedorova with the NIR channel [18]. The impact of each different implementation in the model mentioned above on the D/H cycle is summarized by Figure 1[24]. It shows the H_2O and HDO mixing ratios, and the D/H ratio at 80 km altitude, as computed by the model, and interpolated at the ACS measurements coordinates, for a simulation of reference [REF], where all physical packages (radiatively active clouds, microphysics, kinetics and photochemistry) have been activated, and for all other simulations, in which each physical process stud-

ied has been separately turned off. This study confirms the importance of taking into account these different physical processes to significantly improve the comparison to observations, and it particularly emphasizes the major role of representing the state of supersaturation (see Figure 1). Comparisons of the corresponding D/H ratio profiles between GCM and observations are shown and analysed in the companion paper Rossi et al. 2022[30].
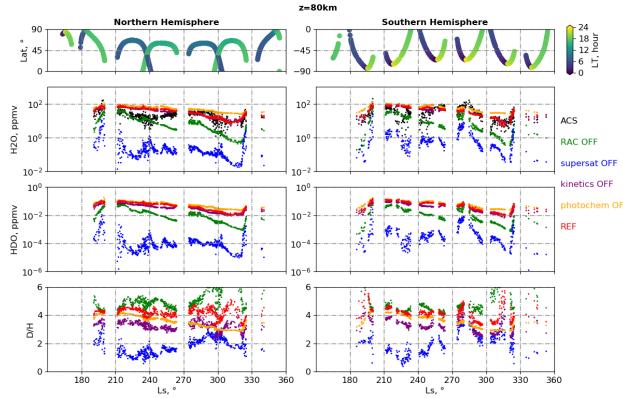

Figure 1: H_2O, HDO and D/H ratio GCM outputs interpolated to the ACS spatial and temporal coordinates at 80 km altitude, as a function of solar longitude (Ls). Left column: northern hemisphere, right column: southern hemisphere. First panel corresponds to the data coverage in latitude and local time. Second row displays the H_2O volume mixing ratio in logarithmic scale. Third row displays the HDO volume mixing ratio in logarithmic scale. Fourth row contains the D/H ratio. GCM outputs are shown for the reference simulation [REF], a simulation in which the radiative effect of clouds has been turned off [RAC OFF], a simulation in which the supersaturation has been turned off [supersat OFF], a simulation in which the effect of kinetics has been turned off [kinetics OFF] and a simulation in which the photochemistry has been turned off [photochem OFF]. ACS water vapor volume mixing ratio are shown in the second row (black dots).

Modeling water cycle during the MY34 GDS

Although the new implementations have considerably improved the comparison with observations in regards to water vapor amount, which has a direct impact on the D/H ratio, some discrepancies remain. In particular, Figures 2 and 3 display the amount of water vapor at three different altitude ranges, respectively at 40, 60, 80 km, and at 80, 100, 110 km, obtained by the model reference simulation compared to the ACS/NIR and ACS/MIR observations[18],[31], still during the second half of MY34. Model results and observations are in good agreement at 40 km, but this is not the case any more

from around 60 km up to the higher altitude ranges, where the model presents much higher amount of water vapor than observations between Ls 210-240° in both Hemispheres, whereas it fails at representing the peak of water vapor observed around Ls 270-300°, in particular in the Southern Hemisphere.
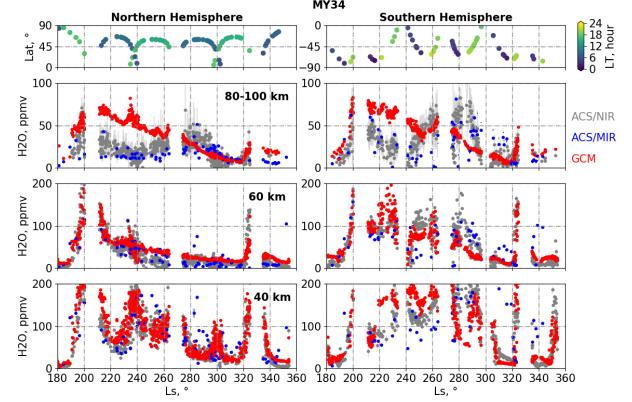

Figure 2: H_2O mixing ratio at 40, 60 and 80 km altitude ranges, as a function of solar longitude (Ls). (red) GCM outputs of the reference simulation interpolated to the ACS spatial and temporal coordinates. (blue) ACS/MIR observations, Belyaev et al. 2021[31]. (grey) ACS/NIR observations, Fedorova et al. 2020[18]
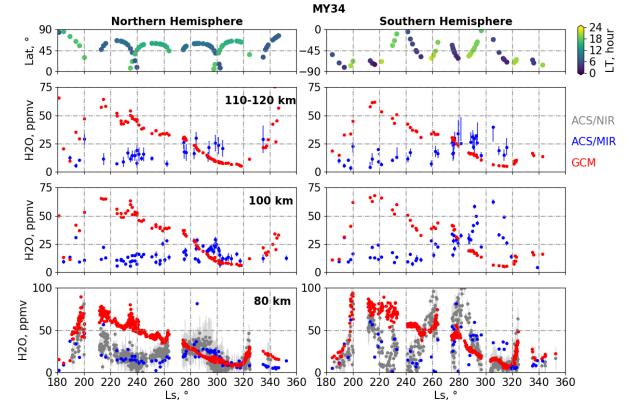

Figure 3: Same layout as Figure 2 at 80, 100 and 110 km altitude ranges.

Discussion

Figure 4 displays GCM H_2O mixing ratio and temperature profiles compared to ACS observations[18] between Ls 235-245°, in the tropics. Although temperature profiles are quite in good agreement, the GCM is clearly showing a wetter atmosphere than observed from around

60 km altitude. Figure 5 is showing some ice mass load profiles measured by Luginin et al. 2021[32] in the same period of time and latitude ranges and compared to the corresponding GCM ouputs. This Figure reveals that water ice clouds observed above 60 km are not reproduced by the model. These comparisons suggest that the model is missing the representation of condensation occuring during the GDS and later on at the upper altitudes. The suspected reason for that is the lack of dust nuclei in the model, as it is well known that GCMs have difficulties to correctly represent the vertical distribution of dust, especially during dusty events, where sub-grid scale convection processes are not well represented. Indeed, Neary et al. 2020[19] and Daerden et al. 2022[16] chose to prescribe the dust profile during the GDS and achieved good comparisons of water vapour amount and D/H ratio profiles.
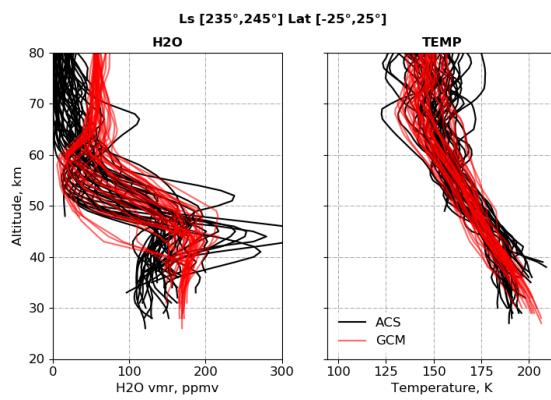

Figure 4: Profiles of water vapor and temperature between Ls = 235-245° and latitude 25°S and 25°N as measured by ACS (black line) and computed by the GCM (red line).
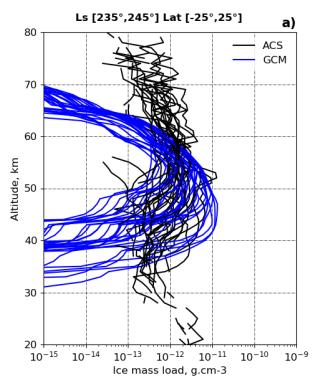
Figure 5: Profiles of water ice mass load between Ls = 235-245° and latitude 25°S and 25°N as measured by ACS (black line) and computed by the GCM (blue line).

Conclusions and perspectives

We have improved the representation of the HDO cycle in the LMD Mars GCM by adapting it to the full water cycle of the model including microphysics and radiative effect of clouds, by completing the modeling of the fractionation by condensation with the effect of kinetics, and by adding the complete photochemistry of HDO and deuterated species. The main impact of these different implementations is the representation of supersaturation state, which considerably improves the comparison of water vapor amount between model results and observations during the "dusty" season of MY34. However, some discrepancies remain in the upper altitude ranges, where the model predicts a much wetter atmosphere than observed in both hemispheres. The poor representation of the dust vertical distribution is suspected to play a huge role in this aspect and will be further investigated. Further results and interpretations on the comparison between model ouputs and TGO/ACS observations will be presented at the conference.

References

[1] Owen et al.: Science, 240 (4860), 1767-1770, 1988

[2] Encrenaz et al.: A&A, 612 , A112, 2018.

[3] Krasnopolsky: Icarus, 257 , 377 - 386, 2015

[4] Villanueva et al.: Science, 348 (6231), 218â^221, 2015.

[5] Cheng et al.: Geophysical Research Letters, 26 (24), 3657-3660, 1999

[6] Krasnopolsky: Icarus, (2), 597-602, 2000.

[7] Fouchet et al.: Icarus, 144 , 114-123, 2000.

[8] Bertaux et al.: Journal of Geophysical Research: Planets, 106 (E12), 32879-32884, 2001.

[9] Rossi et al.: grl , 48 (7), e90962, 2021.

[10] Forget et al.: JGR, 104:24,155–24,176, 1999.

[11] Montmessin et al.: Journal of Geophysical Research, 2005.

[12] Vandaele et al.: Space Science Reviews, 214 (5), 80, 2018.

[13] Vandaele et al.: Nature, 568 (7753), 521-525, 2019.

[14] Korablev et al.: Space Science Reviews, 214 , 7, 2018.

[15] Korablev et al.: Nature, 568 (7753),517-520, 2019.

REFERENCES

[16] Daerden et al.: Journal of Geophysical Research (Planets), 127 (2), e07079, 2022.

[17] Aoki et al.: Journal of Geophysical Research (Planets), 124 (12), 3482-3497, 2019.

[18] Fedorova et al.: Science, 367 (6475), 297-300, 2020.

[19] Neary et al.: Geophysical Research Letters, 47 (7), e84354, 2020.

[20] Chaffin et al.: Nature Astronomy, 5 , 1036-1042, 2021.

[21] Madeleine et al.: Journal of Geophysical Research (Planets), 116 , 11010.669, 2011

[22] Montabone et al.: Icarus.2014.12.034700, 2015.

[23] Montabone et al.: Journal of Geophysical Research: Planets, n/a(n/a), e2019JE006111, 2020.

[24] Vals et al.: Journal of Geophysical Research (Planets), under revision, 2022.

[25] Madeleine et al. : Geophys. Res. Lett., 39 , 23202, 2012.

[26] Navarro et al.: Journal of Geophysical Research (Planets), 2014.

[27] Lefèvre et al.: Journal of Geophysical Research (Planets), 126 (4), 2021.

[28] Cheng et al.: Journal of Chemical Physics, 120 (1), 224-229, 2004

[29] Chung et al.: Nuclear Instruments and Methods in Physics Research A, 467 (2002), 1572-1576, 2001.

[30] Rossi et al.: Journal of Geophysical Research (Planets), under revision, 2022.

[31] Belyaev et al.: Geophysical Research Letters, 48 (10), 2021.

[32] Luginin et al.: Journal of Geophysical Research (Planets), 125 (11), e06419, 2020.